J Fluoresc (2012) 22:1101–1111
DOI 10.1007/s10895-012-1049-x

ORIGINAL PAPER

Fluorescence Characteristics and Inclusion of ICT Fluorescent Probe in Organized Assemblies

Tarek A. Fayed · Mohammed A. El-morsi · Marwa N. El-Nahass

Received: 13 October 2011 / Accepted: 19 March 2012 / Published online: 18 April 2012

Abstract The inclusion behavior of an intramolecular charge transfer (ICT) fluorescent probe namely; 2-[3-(4-dimethylamino-phenyl)-allylidene]-tetralone (DMAPT) in organized assemblies of aqueous micellar, α- and β-cyclodextrins (CDs) and bovine serum albumin (BSA) pockets have been studied using steady-state absorption and fluorescence spectroscopy. The fluorescence characteristics (energy and intensity) of DMAPT are highly sensitive to the properties of the medium. The ICT maximum is strongly blue-shifted with a great enhancement of the fluorescence intensity upon addition of different surfactants, confirming the solubilization of DMAPT in the hydrophobic micellar assembly. In addition, the fluorescence of DMAPT is more sensitive to the nature and concentration of the added CDs. In α- or β-CD solutions, the fluorescence intensity increases strongly (by 6 and 23 orders of magnitude, respectively). Upon encapsulation in the CD cavity, the molecular flexibility decreases due to the geometrical restrictions of the CD nanocavity which decreases the non radiative transition via the free rotation around the single and/or double bonds of the butadiene bridge. This was supported by finding that the fluorescence quantum yield of DMAPT increases with increasing the viscosity of the medium. The binding constants of DMAPT with micelles, α- and β-CD solutions have been calculated and were found to be highly dependent on the nature of the used surfactants or CDs. The thermodynamic parameters have been also determined and the difference in magnitude between the formed α- and β-CD-DMAPT inclusion complexes is discussed on the basis of the cavity size. Finally, the binding constant of DMAPT with bovine serum albumin was calculated, indicating the relative stability of the DMAPT–BSA complex. The energy transfer distance between BSA as a donor and DMAPT as an acceptor was obtained following the fluorescence quenching of BSA by DMAPT, via resonance mechanism as a quencher.

Keywords ICT fluorescence · Micelle · Cyclodextrin Inclusion complex · Energy transfer · Bovine serum albumin

T. A. Fayed (✉) · M. A. El-morsi · M. N. El-Nahass
Department of Chemistry, Faculty of Science, Tanta University, 31527, Tanta, Egypt
e-mail: tfayed2003@yahoo.co.uk

M. N. El-Nahass
e-mail: marwacu@yahoo.com

Introduction

Self-assembly of organic molecules results in many interesting and complex structures as, folded proteins or supramolecular structures of micelles and cyclodextrins [1–3]. Self-assembly is mainly governed by the delicate balance between hydrophobic and hydrophilic interaction. In an organized assembly, the active chemical species remains confined in a small volume, a few nm in size. Such confinement imposes restrictions on the free motion of the probe and the confined solvent molecules. Several authors have discussed the hydrophobic effect which causes binding of organic probes with micelles, cyclodexrins and bovine serum albumin in aqueous medium on many photophysical processes [4–6].

Micelles are being extensively studied as rudimentary models for biological systems [7, 8]. Attention has been paid to the micellar activities on the nature and characteristics of different photophysical and photochemical processes [9]. Upon inclusion, a molecule will experience a different environment inside the microheterogeneous

structure of micelle, than that of bulk solvents for e.g., polarity, viscosity and diffusion of water molecules changes on moving towards the core of the micelle. Knowledge of the properties of water at interfaces of organized assemblies, at the microscopic level, is a prerequisite for understanding the mentioned effects. This is because interfacial water molecules are involved in solvation of reactants, transition states, surfactants head-group and counter ions as well as in proton transfer [10].

Cyclodextrins (CDs) are donut-shaped cyclic oligosaccharides consisting of six or more α-(1,4)-linked D-glucopyranose units, are able to form inclusion complexes (host–guest complexes) with a wide variety of guest organic molecules possessing suitable polarity and dimension characteristics [11]. Complexation is governed by various types of interactions, including geometrical steric factors, hydrophobic interactions, hydrogen bonding, and London dispersion forces [12]. Cyclodextrin inclusion complexes can be studied by a number of experimental techniques, including UV/visible spectroscopy [13], NMR spectroscopy [14], calorimetry, circular dichroism [15], X-ray crystallography [16], and fluorescence spectroscopy [17]. In addition to these experimental methods, computational studies have also been widely applied to cyclodextrin inclusion [18]. In the case of UV/visible and fluorescence spectroscopy, a change in absorption and emission maxima of the guest is observed. Of these, fluorescence is the most sensitive, as it requires the lowest concentration of sample, and furthermore for highly polarity-sensitive guests, exhibits by far the largest effects upon inclusion. It is thus an excellent technique for studying cyclodextrin inclusion phenomena.

Bovine serum albumin (BSA) is consists of varieties of amino acid residues and on the basis of the distribution of the disulfide bridges and of the amino acid sequence, it seems possible to regard BSA as composed of three homologous domains linked together. Serum albumin often increases the apparent solubility of hydrophobic drugs in plasma and modulates their delivery to cells in vivo and in vitro. Consequently, it is important to study the interactions of drugs with this protein. The effectiveness of drugs depends on their binding ability [19]. Quenching measurements of albumin fluorescence is an important method to study the interactions of compounds with proteins [20]. It can reveal accessibility of quenchers to albumin's fluorophores, help to understand albumin binding mechanisms to compounds and provide clues to the nature of the binding phenomenon [21].

Photoinduced intramolcular charge transfer (ICT) interaction is currently one of the most attractive optics of interest as a primary function for photoelectronic devices [22] as well as a basic mechanism of biological processes [23] and chemical-energy conversion [24]. Recently, the photophysical properties of molecules showing ICT or twisted ICT (TICT) have been studied in CDs-aqueous media [25, 26]. Ketocyanine dyes form a class of compounds whose absorption and emission characteristics are strongly dependent on their environments [27, 28]. Hence they are potentially used as indicators for studying solvation interactions in homogeneous and microheterogeneous media. Thus, the spectroscopic and photophysical study of these molecular systems in organized assemlies and serum albumin is very helpful for a better understanding of the nature of inclusion and biodistribution of the dye inside the living cells.

In the present study, the absorption and emission characteristics of a ketocyanine analogue namely; 2-[3-(4-dimethylamino-phenyl)-allylidene]-tetralone (DMAPT) which exhibits intramolecular charge transfer emission (ICT) have been studied in organized assemblies of micelles (SDS, CTAB and, TX-100), cyclodextrins (α, β-CD's) and bovine serum albumin (BSA). This is to give insights on the ICT emission and inclusion behavior of such a ketocyanine in these media and determine the inclusion parameters as well as exploring its probing ability to characterize the properties of these media.

Experimental

The investigated ketocyanine namely; 2-[3-(4-dimethylamino-phenyl)-allylidene]-tetralone (DMAPT) was synthesized and characterized as described in a previous work [29]. The used surfactants are sodium dodecyl sufate (SDS, BDH), cetyltrimethylammonium bromide (CTAB, BDH) and Triton X-100 (TX-100, Aldrich) as example of anionic, cationic and neutral micelles, respectively, were used as supplied. α- and β-cyclodextrins (Aldrich), bovine serum albumin (BSA, Sigma) were used as received. Bidistilled water was used for preparation of solutions.

Steady-state absorption and emission spectral measurements were carried out using a Shimadzu UV-3101PC scanning spectrophotometer and a Perkin–Elmer LS 50B spectrofluorometer, respectively. Both techniques are equipped with temperature controlled cell holders. The temperature of the cell compartments was kept constant by circulating water using an Ultrathermostate Fisher Scientific (Pittsburgh, PA 9000).

For spectral measurements, the concentration of DMAPT was kept constant at 2×10^{-5} M, while the surfactant concentration was varied within the range $0.2–45.0\times10^{-3}$ M, depending on the nature of the used surfactant. In the case of α and β-CD, the concentration ranges from 3×10^{-3} to 2.7×10^{-2} M. The fluorescence spectra of DMAPT in CD's solutions were measured at four different temperatures within the range from 15 to 45 °C. For spectral measurements at different temperatures, the solution was left in the thermostated cell holder for

at least 10 min before recording the spectra to maintain thermal equilibrium.

A stock solution of BSA (1,000 μg/ml) was prepared by dissolving 0.025 g in 25 ml using bidistilled water. For spectral measurements, different volumes of BSA (0.1–3 ml) were added to 0.1 ml of 10^{-3} M DMAPT mixed thoroughly into 5 ml volumetric flask, then diluted with bidistilled water.

In order to study the fluorescence quenching of BSA using DMAPT as a quencher in aqueous solution, different concentrations of DMAPT (0.0–5.4×10^{-4} M) were added to 1 ml of 100 μg/ml BSA into a 5 ml volumetric flask. The samples were excited at 280 nm while the emission spectrum was recorded in the range 285–450 nm in the absence and presence of DMAPT.

Results and Discussion

Spectral Behavior and Solublization of DMAPT in Micellar Solutions

The spectral properties of DMAPT have been studied in CTAB, TX-100 and SDS micellar solutions. Figure 1 shows the absorption and fluorescence spectra of DMAPT in the absence and presence of surfactants at concentrations higher than critical micelle concentrations, and the corresponding spectral data are collected in Table 1. The 437 nm absorption band of DMAPT in water is red shifted by 4–23 nm in micelles, depending on the nature of the used surfactants (whether neutral, cationic or anionic). The spectral shift is consistent with solublization of DMAPT molecules in the surfactant micelles.

Contrarily, the fluorescence band of DMAPT observed at 597 nm in water is blue-shifted on adding SDS, CTAB and TX-100 (by 8, 11 and 22 nm, respectively). This shift is accompanied by a great enhancement of fluorescence intensity (Fig. 2) which can be rationalized in terms of binding of this hydrophobic probe to the less polar sites in micelles. Due to the ICT characters of the excited singlet state of DMAPT, lowering the polarity of the medium destabilizes the excited state and leads to blue shift of the fluorescence maximum [30]. In CTAB and SDS micellar solutions, the dipolar excited DMAPT molecules will be transferred to a less polar hydrophobic environment near the surface of the micelle. This is indicated by the calculated polarity of these micelles as sensed by DMAPT (the polarity of the microenvironment of the used micelles expressed as $E_T(30)$ are 45.4 and 45.6 kcal/mole for CTAB and SDS, respectively). However, in Triton-X-100, the calculated $E_T(30)$ is 43.6 kcal/mole, indicating that the DMAPT molecules reside in a more hydrophobic less polar environment relative to the other surfactants. The empirical solvent polarity parameter $E_T(30)$ of the micelle environment was calculated utilizing the correlation between fluorescence energy (E_F) of DMAPT in different solvents and the empirical solvent polarity parameter of

Table 1 Spectral maxima, critical micelle concentrations (CMC) and determined polarity $E_T(30)$ of the different micelles as well as the binding constant of DMAPT with micelles

Micellar media	λ^a_{max} (nm)	λ^f_{max} (nm)	CMC × 10^{-3} mole/l	$E_T(30)$	$K \times 10^5$ L mole^{-1}
Water	437	597	–	48.19	–
CTAB	454	586	1.0 (0.9) [a]	45.4	1.37
TX- 100	441	575	0.46 (0.3) [a]	43.6	0.73
SDS	460	589	8.3 (8.0) [a]	45.6	0.66

(a) Values were determined by using 4-aminophthalimide as a probe [33]

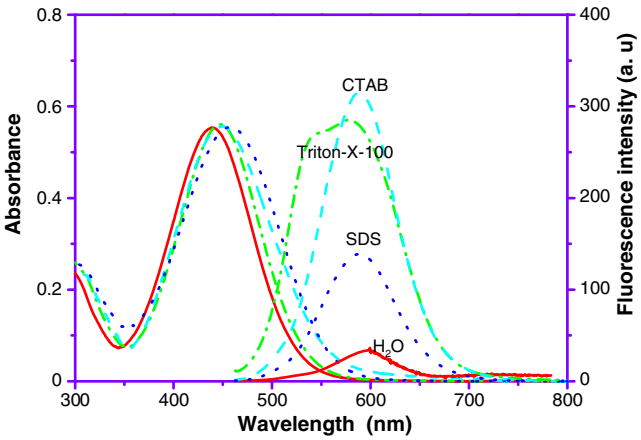

Fig. 1 Absorption and fluorescence spectra of DMAPT in water (—), CTAB (——), Triton-X-100 (-.-.-.), and SDS (…..) micellar solutions

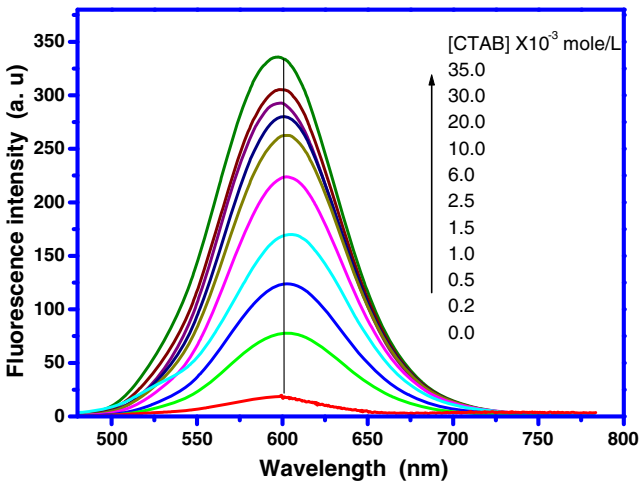

Fig. 2 Fluorescence spectra of DMAPT measured in CTAB micellar solutions, λ_{ex} = 430 nm. The surfactant concentrations are shown in the Figure

Dimorth-Reichardt [31] as reported in a previous work [32], according to the following equation:

$$E_F = 70.7 - 0.48\ E_T(30) \quad (1)$$

Long-chain amphiphilic molecules form micellar aggregates, in aqueous solutions, above certain concentration called critical micelle concentration, CMC. Herein, DMAPT has been employed to determine the CMC for the used surfactants. The CMC values were calculated from variations of the relative fluorescence intensities (I_f/I_f^o) with surfactant concentrations as shown in Fig. 3. The obtained values given in Table 1 are in good agreement with those determined by using other known probes [33].

A quantitative estimate of the binding constant (K) for the equilibrium, representing dye-/micelle interaction, can be calculated by using the equation proposed by Almgren et al. [34]. For the equilibrium

$$D + M \leftrightarrow D....M$$

Where D and M represent dye molecule and micelles respectively, for which

$$(I_m - I_\circ)/(I_t - I_\circ) = 1 + (K[M])^{-1} \quad (2)$$

where $I_\circ$, I_t, and I_m are the fluorescence intensities of the probe in the absence of surfactant, at an intermediate concentration [M] and under complete micellization, respectively. K is the binding constant. The micellar concentration [M] is determined by;

$$[M] = (S - CMC)/N \quad (3)$$

Where S represents the surfactant concentration under experimental condition and N is the aggregation number of the micelles. The N values were taken as 60, 62 and 143 for CTAB, SDS and TX-100, respectively [35]. According to equation 2, the plots of $(I_m - I_\circ)/(I_t - I_\circ)$ versus 1/[M] are linear as shown in Fig. 4 where the K values have been determined from the slopes and collected in Table 1. The binding constant for inclusion of DMAPT in CTAB is about two times greater than that in SDS. This reflects the role of the electrostatic interaction between the dye and the micelle. In CTAB micellar medium, the positively charged head groups would interact favorably with the negatively charged carbonyl oxygen of the dye, particularly in the excited state. While in SDS, the negatively charged head groups will interact with the positively charged $-NMe_2$ group and suffers some steric interactions thus leading to relatively weak binding as indicated by the relatively small inclusion constant.

Inclusion of DMAPT CDs Cavity

The absorption spectra of DMAPT change upon complexation with α- and β-CD's, Fig. 5. The absorption of DMAPT at 437 nm in water increases upon addition of α- or β-CD (0.0–2.7×10^{-2} M) with pronounced red shift and appearance of a shoulder around 570 nm. In β -CD, an isosbestic point at 474 nm appears with increasing of the absorbance of the band at 450 nm on the expense of the absorbance of the shoulder. However in α–CD, no isosbestic point was formed, where the spectrum rises up with the concentration of CD. This behavior is attributed to the enhanced dissolution of the guest DMAPT molecule through the hydrophobic interaction with the nonpolar cavities of CDs and formation of inclusion complexes. The change of the measured absorbance with the CD concentration is shown as inset in Fig. 5.

Figure 6 shows steady state fluorescence spectra of DMAPT in water containing different concentrations of α-

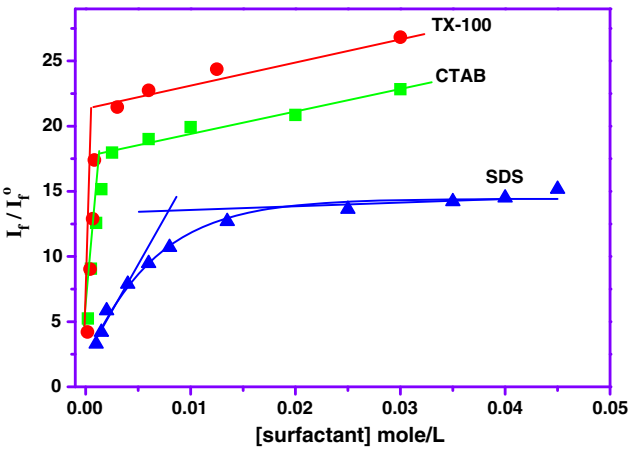

Fig.3 Variation of the relative fluorescence intensity of DMAPT as a function of CTAB (*black square*), Triton-X-100 (*black circle*) and SDS (*black up-pointing triangle*) concentration

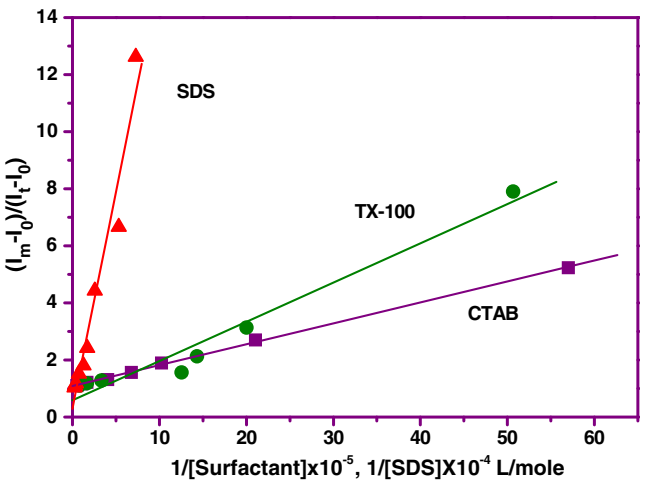

Fig. 4 Plots of $(I_m - I_0)/(I_t - I_0)$ against $[M]^{-1}$ for DMAPT in surfactants

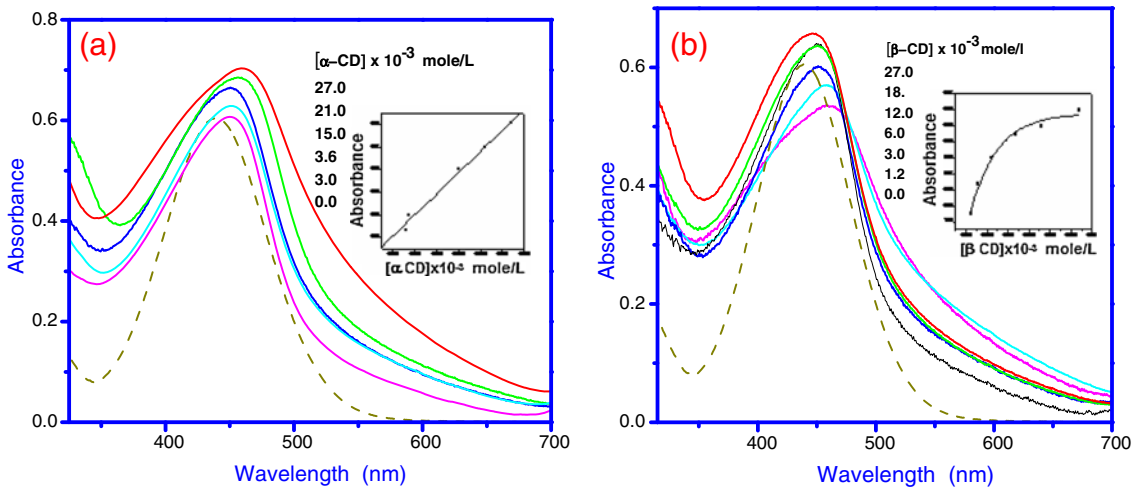

Fig. 5 Absorption spectral changes of DMAPT on adding different concentrations of (**a**) α-CD and (**b**) β-CD. Inset: the change in the absorption maximum of DMAPT with increasing the concentration of CDs

or β-CD. The Figure shows that the fluorescence spectra of DMAPT are more sensitive to the nature and concentration of the added CD. While DMAPT is weakly fluorescent in water, on addition of α- or β-CD, the fluorescence intensity increases strongly (6 and 23 orders of magnitude, respectively). The enhancement of the fluorescence intensity is due to decrease in non radiative transition via the free rotation around the single and/or double bonds of the butadiene bridge. Upon encapsulation in the CD cavity, the molecular flexibility decreases due to the geometrical restriction of the CD nanocavity. This was supported by finding that the fluorescence quantum yield of DMAPT increases with increasing the viscosity of its microenvironment. The fluorescence quantum yield increases 12 times on going from methanol to glycerol as a solvent (ϕ_f = 0.023 and 0.29, respectively). Additionally, the fluorescence quantum yield decreases from 0.29 at 26 °C to 0.11 as the temperature is raised to 65 °C in glycerol.

In β-CD, dual emission is observed where a new band builds up around 558 nm. The observed dual emission can be explained on the basis of two probabilities, firstly, the long wavelength fluorescence is due to free DMAPT molecule, while the band at shorter wavelength can be attributed to the formation of inclusion DMAPT-β-CD complex. Secondly, the dual emission is due to formation of two inclusion complexes via two different modes of inclusion of DMAPT in the CD cavity. The difference in spectral change of DMAPT on adding α- or β-CD in aqueous solution suggests that the structural geometry of the [DMACA-CD] inclusion complexes is different in terms of orientation of the guest molecule. DMAPT can enter CD longitudinal in two ways, as shown in Scheme 1. If the inclusion complex is

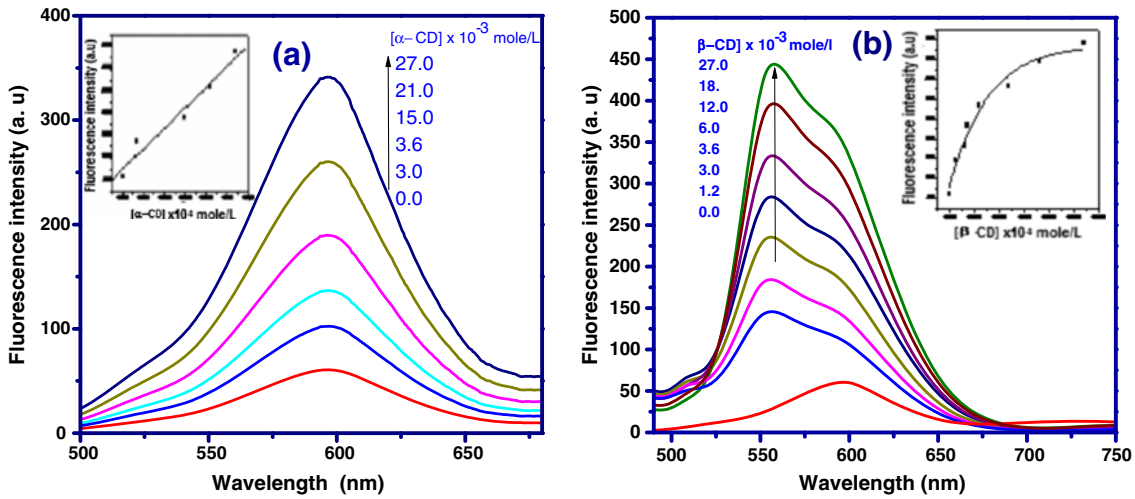

Fig. 6 Fluorescence spectral changes of DMAPT (2×10^{-5} M) on adding different concentrations of (**a**) α-CD and (**b**) β-CD. Inset: the change in the emission maximum of DMAPT with increasing the concentration of CDs

Scheme 1 The proposed structures of the inclusion complexes of DMAPT with α- and β-CDs

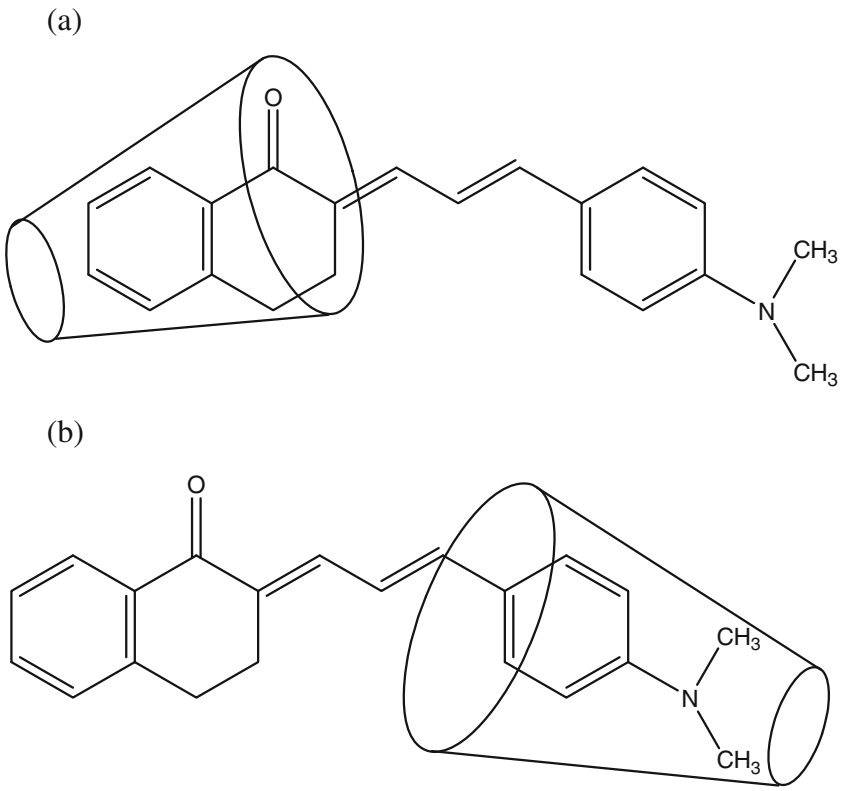

formed as shown in Scheme 1a with the -NMe_2 group reside outside the host cavity in the bulk water phase thus will experience the same kind of solvation as in the aqueous medium, consequently no shift in the fluorescence maximum is expected. In this mode of complexation the tetralone moiety of DMAPT will be present inside the CD cavity with the carbonyl group are placed close the wider rim of the CD near the -OH groups. In the other mode of solvation, Scheme 1b, the -NMe_2 group would be buried in the hydrophobic cavity and then the bulk water are not available to solvate it, so, blue shift in the emission band is expected.

In α–CD where the cavity size is small (diameter is 5.3 A° [36]) it allows inclusion of the DMAPT molecule via the mode with the tetralone moiety inside the cavity (Scheme 1a). However, the probability of inclusion of DMAPT molecules with the –NMe_2 group inside the α–CD cavity is hindered by the twisted geometry of the dimethylaniline moiety (the torsion angle of the phenyl ring within the amino group is 59.4° [32]). This is consistent with the observed no shift of the fluorescence maxima in α–CD. In the case of β-CD the cavity is large enough to allow DMAPT to interact with the CD via the previously mentioned two modes of inclusion. By comparison with the results in α–CD, the observed dual emission in β-CD is due to the formation of inclusion complexes via the tetralone moiety inside the β-CD cavity with the carbonyl group near the –OH groups of the wider rim (responsible for the fluorescence at 597 nm). On the other hand, the appearance of the short wavelength fluorescence band at 558 nm is due to formation of inclusion complex with -NMe_2 inside the hydrophobic β-CD cavity. In fact, attribution of the fluorescence band at longer wavelength (597 nm) to emission from the free DMAPT molecules is ruled out due to the finding that the fluorescence intensities at 558 and 597 nm increase monotonically (ratio at both wavelengths is ≈1.3 for β-CD concentrations 1.2 and 27.0×10^{-3} M). In addition, the fluorescence is leveled off at higher β-CD concentrations as shown in the inset of Fig. 6.

To get information about the stiochiometry and stability of the formed DMAPT-CD complexes, the Benesi–Hildebrand [37] double reciprocal plots were tested according to the following equation;

$$\frac{1}{F-F_0}=\frac{1}{F_\infty-F_0}\cdot\frac{1}{K_{in}[CD]_0}+\frac{1}{F_\infty-F_0} \quad (4)$$

Where F_0 and F_∞ denote the fluorescence intensity of DMAPT in the absence of α- or β-CD's and when all molecules are complexed with α- and β-CD's, respectively. F is the fluorescence intensity measured at each tested $[CD]_0$, and K_{in} is the inclusion constant of the formed host–guest complex.

A typical linear double reciprocal plot was established in the concentration range 1.2–27.0×10^{-3} M of α- and β-CD's, Fig. 7. The possibility of formation of a 2: 1 (host: guest) complex is ruled out as the plot of $1/(I-I_0)$ vs. $1/[CD]^2$ are non

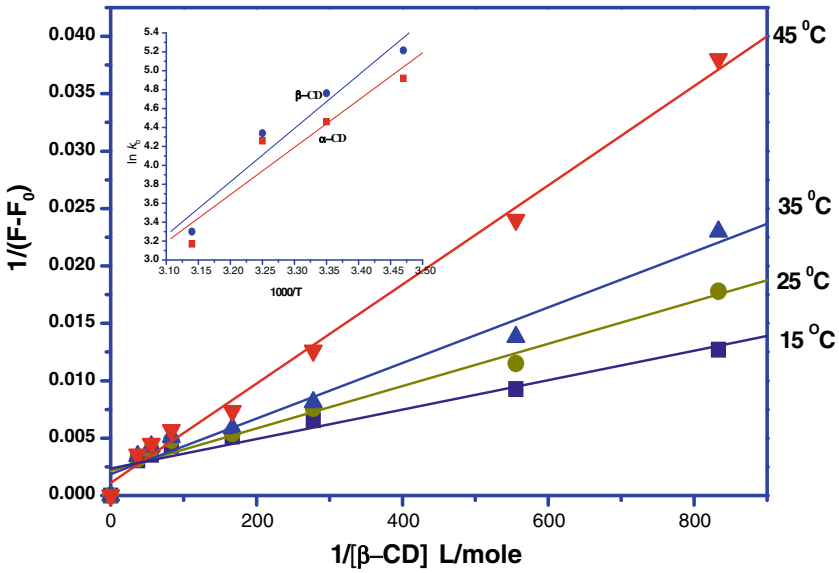

Fig. 7 Benesi-Hildebrand plots for the emission of DMAPT in β-CD solutions at different temperatures. Inset: are the Vant Hoff plots of logarithmic inclusion constants of DMAPT in CDs

linear, supporting the assumed 1:1 inclusion of the DMAPT in α- and β-CD's. The binding constants were calculated, Table 2. The calculated values for the inclusion complex with β-CD are larger than those for α-CD (at 25 °C, K_{in} = 117.1 and 86.7 dm^3 mole^{-1}, respectively). This suggests the stronger hydrophobic interactions experienced by DMAPT with β-CD compared to α-CD, and supports the role of cavity size in determining the stability of the formed complex.

To explore the thermodynamic of the binding process, the temperature dependence of the binding constant was also studied where it was found that K_{in} decreases with increasing the temperature. The thermodynamic parameters were determined by applying Van't Hoff equation [38].

$$\ln(K_{in}) = -\frac{\Delta H^0}{R}\left[\frac{1}{T}\right] + \frac{\Delta S^0}{R} \tag{5}$$

Where R is the gas constant, T is the absolute temperature, ΔH^0 and ΔS^0 are the enthalpy and entropy of activations, respectively. Representative plot is shown in the inset of Fig. 7. The corresponding enthalpy ΔH° and entropy ΔS° changes are obtained from the slope and intercept of the plot, respectively, while the Gibbs free energy change is calculated from the following equation:

$$\Delta G^o = -RT \ln K_{in} \tag{6}$$

The calculated thermodynamic parameters are collected in Table 2. The negative sign of the obtained ΔH^o values (−40.86 and −46.19 kJ/mole for α- and β-CD's, respectively) may be accounted for the hydrophobic interactions between the fluorophore and the cavity of CD [39]. The negative values indicate that the inclusion process is an exothermic and enthalpy controlled. The difference in magnitude between the parameters calculated for α-CD and β-CD complexes is discussed on the bases of the cavity size, the higher entropy values possibly results from the release of the high energy water molecules from the host cavity during the encapsulation of the dye into the host cages [40]. Upon complex formation these water molecules are expelled and reform their hydrogen bond network. The situation is different in the larger β-CD cavity where water has the possibility of a more extensive hydrogen bonding. The kinetics for α-CD is slow, associated

Table 2 Binding constants (k_{in}) and thermodynamic parameters of complexation of DMAPT with α- and β-CDs at different temperatures

Media	λ^a_{max} (nm)	λ^f_{max} (nm)	Temperature °C	K_{in} (dm^3 mole^{-1})	-ΔH° (kJ/mole)	-ΔS° (J/mole)	-ΔG° (kJ/mole)
α-CD	459	595	15	137.25	40.86	100.76	10.76
			25	86.72			
			35	70.92			
			45	23.98			
β-CD	449	557	15	184.1	46.19	116.46	11.62
			25	117.1			
			35	76.79			
			45	25.46			

with high activation energies for both association and dissociation of the complex [41].

The Interaction of DMAPT with BSA

Gradual addition of BSA resulted in an initial decrease in the absorption band of DMAPT at 430 nm followed by an increase in the absorbance with almost no shift in the absorption maximum, Fig. 8. The room temperature fluorescence spectrum of DMAPT in water is characterized by a broad and structurless charge transfer band with a maximum around 597 nm. However, on addition of BSA, the fluorescence intensity increases strongly with a remarkable blue shift to 581 nm at 600 μg/ml BSA, Fig. 9. Inclusion of DMAPT molecules within the hydrophobic less polar pockets of protein (BSA) leads to destabilization of the ICT excited state and consequently, blue shift of the fluorescence maximum. The absorption and emission spectral changes infer a binding interaction between the dye and the protein.

The use of dye as model of drug and therapeutic agent is basically dependent on its binding ability towards the protein that can also influence their stability and toxicity during the chemotherapeutic process. So, the DMAPT–BSA complex may be suggested as a model for giving insights into drug–protein interactions. In order to assess the binding interaction between DMAPT and the albumin protein, the binding constant has been determined from the fluorescence data following the modified Benesi–Hildebrand equation as follows;

$$1/\Delta F = 1/\Delta F_{max} + (1/K[BSA])(1/\Delta F_{max}) \quad (7)$$

Where $\Delta F = F_x - F_o$ and $\Delta F_{max} = F_\infty - F_o$ where F_o, F_x and F_∞ are the fluorescence intensities of DMAPT in the absence of protein, at an intermediate protein concentration, and at a concentration for inclusion of all DMAPT, respectively, K being the binding constant and $[L]$ is the free protein concentration. Plot of $1/\Delta F$ against [L] gives a straight line, Fig. 9, thereby justifying the validity of Eq. (6) and hence confirming the interaction between the dye and the protein. The value of K, thus obtained at 300°K is 7.0×10^3 L mole^{-1} is relatively high and indicates stability of the formed dye–protein complex [42].

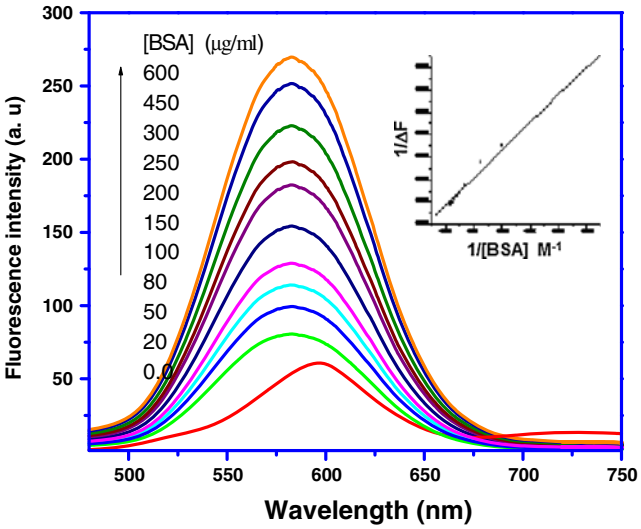

Fig. 9 Emission spectra of DMAPT as a function of BSA concentration (λ_{ex} =460 nm). Inset: is the Benesi-Hildebrand plots for the binding of DMAPT in BSA

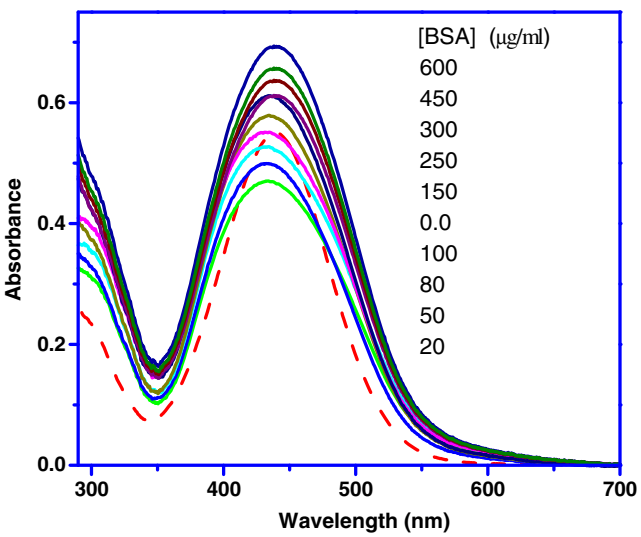

Fig. 8 Absorption spectra of DMAPT recorded in the presence of different concentrations of BSA

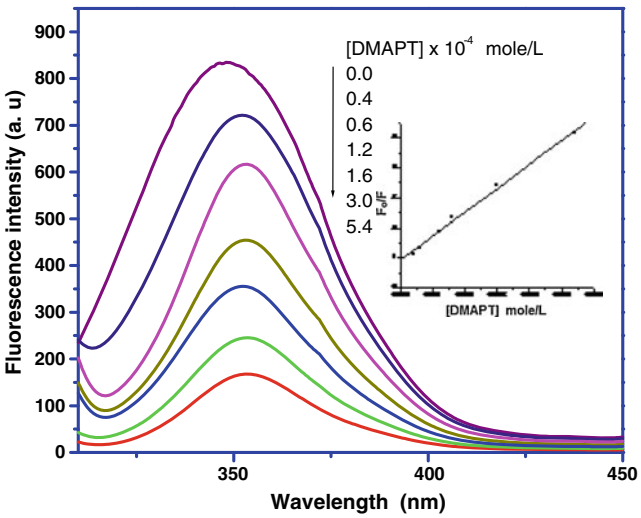

Fig. 10 Fluorescence spectral changes of BSA on adding different concentrations of DMAPT at λ_{ex} = 280 nm. Inset: is the Stern-Volmer plots for the quenching of BSA fluorescence by DMAPT

Fluorescence Quenching of Serum Albumin by DMAPT

The fluorescence of BSA was efficiently quenched by addition of DMAPT, Fig. 10, without change of the band profile indicating the absence of emission from new species.

The quenching mechanism of BSA fluorescence by DMAPT was investigated using the Stern–Volmer equation [43]:

$$F_o/F = 1 + K_q\tau_o[Q] = 1 + K_{SV}[Q] \quad (8)$$

Where F_o and F represent the fluorescence intensities in the absence and presence of the quencher, K_q is the bimolecular quenching rate constant, K_{SV} is the Stern–Volmer quenching constant, τ_o is the average lifetime of BSA without quencher which was taken as 10^{-8} s [44], and [Q] is the concentration of the quencher which is DMAPT. It has been found that the Stern-Volmer plot is linear, Fig. 10. As the absorption spectrum of DMAPT and the fluorescence spectrum of BSA are overlapped, Fig. 11, analysis of the fluorescence intensity is treated considering the energy transfer mechanism. For the DMAPT–BSA system, the values of K_{SV} and K_q are 0.794×10^4 M^{-1} and 0.792×10^{12} L mole^{-1} s^{-1}, respectively, with the K_q value 100 factor greater than the calculated diffusion controlled constant ($K_{diff} = 0.64\times10^{10}$ L mole^{-1} s^{-1} [45]). The higher value of K_q is consistent with the energy transfer over relatively large distances as a possible quenching mechanism. Energy transfer according to the long-range dipole-dipole interaction (Forster mechanism) may give rise to K_q values above the diffusion limit [46].

The importance of the Förster resonance energy transfer in biochemistry is that the efficiency of transfer can be used to evaluate the distance between the ligand and the tryptophan residues responsible of the natural intrinsic fluorescence of proteins. According to Förster's non-radiative energy transfer theory [47], the rate of energy transfer depends on: (i) the relative orientation of the donor and acceptor dipoles, (ii) the extent of overlap of the fluorescence emission spectrum of the donor with the absorption spectrum of the acceptor, and (iii) the distance between the donor and the acceptor. The energy transfer efficiency (E) is related to the critical energy transfer distance, R_0, as described in the following equation:

$$E = 1 - F/F_o = R_o^6/R_o^6 + r_o^6 \quad (9)$$

Where F and F_o are the fluorescence intensities of BSA in the presence and absence of dye, r_o is the distance between acceptor and donor and R_0 is the critical distance when the transfer efficiency is 50 %. R_0^6 is calculated using the equation:

$$R_0^6 = 8.8\times10^{-25}K^2N^{-4}\Phi J \quad (10)$$

Where K^2 is the spatial orientation factor between the emission dipole of the donor and the absorption dipole of the acceptor. The dipole orientation factor, K^2, is the least certain parameter in the calculation of the critical transfer distance, R_0. Although theoretically K^2 ranges from 0 to 4, the extreme values require very rigid orientations. If both the donor and acceptor are tumbling rapidly and free to assume any orientation, K^2 equals 2/3. If only the donor is free to rotate, K^2 can vary from 1/3 to 4/3 [43]. N is the refractive index of the medium, Φ the fluorescence quantum yield of the donor and J is the overlap integral of the fluorescence emission spectrum of the donor and the absorption spectrum of the acceptor given by:

$$J = \sum F(\lambda)\varepsilon(\lambda)\lambda^4\Delta\lambda / \sum F(\lambda)\Delta\lambda \quad (11)$$

Where F(λ) is the fluorescence intensity of the fluorescent donor at wavelength λ which is dimensionless, ε(λ) is the molar absorption coefficient of the acceptor at wavelength λ. J can be evaluated by integrating the spectra in Fig. 11. The calculated value of J was 3.343×10^{-15} cm^3 L mole^{-1}. It has been reported for BSA that $K^2 = 2/3$, $\Phi = 0.15$ and N=1.36 [48]. The values of R_o and r_o were 2.1 and 1.66 nm. These values are less than the common value (8 nm) [49], which indicate that the fluorescence quenching of BSA was also a non-radiative transfer process. Furthermore, the distances obtained by this way agree well with literature values of substrate binding to BSA at site IIA [50].

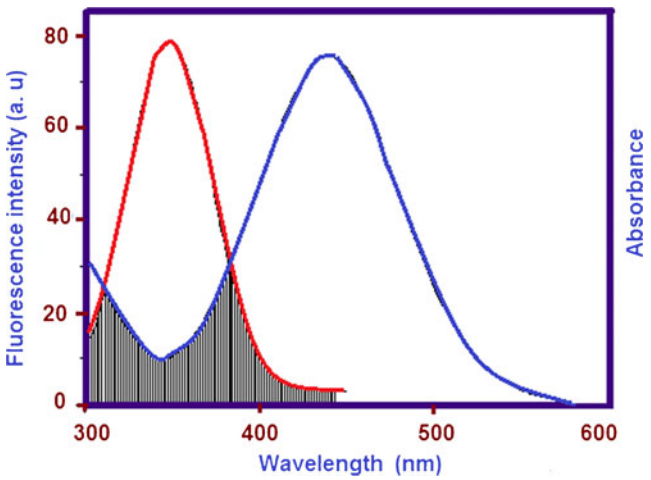

Fig. 11 Overlap between the fluorescence spectrum of BSA and the absorption spectrum of DMAPT

Conclusion

The obtained results, suggest that the ICT fluorescence of DMAPT could be a potential probe for the properties of the investigated organized assemblies to sense and characterize their microenviromental polarity, critical micelle concentrations of surfactants. Also, it could determine the difference in the size of the cavity of CDs and the binding site of the hydrophobic BSA pockets.

References

1. David SS, O'Shea LV, Kundu S (2007) Base-excision repair of oxidative DNA damage. Nature 447:941–950. doi:10.1038/nature05978
2. Zong C, Papoian AG, Ulander J, Wolynes GP (2006) Role of topology, nonadditivity, and water-mediated interactions in predicting the structures of alpha/beta proteins. J Am Chem Soc 128 (15):5168–5176. doi:10.1021/ja058589v
3. Bhattacharyya K (2008) Nature of biological water: a femtosecond study. Chem Comm 25:2848–2857. doi:10.1039/B800278A
4. Par WJ, Park HK (1994) Inclusion of (aminostyryl)-1-methylpyridinium dyes by β-cyclodextrin and its use for fluorescent-probe studies on association of cationic and neutral molecules with β-cyclodextrin. J Incl Phenom Mol 17(3):277–290. doi:10.1007/BF00708787
5. Doroshenko OA, Sychevskaya BL, Grygorovych VA, Pivovarenko GV (2002) Fluorescence probing of cell membranes with azacrown substituted ketocyanine dyes. J Fluoresc 12(3):455–464
6. Singh BR, Mahanta S, Guchhait N (2008) Study of interaction of proton transfer probe1-hydroxy-2-naphthaldehyde with serum albumins: a spectroscopic study. J Photochem Photobiol B Biol 91(1):1–8. doi:10.1016/j.jphotobiol.2007.12.006
7. Fendler HJ (1982) Membrane mimetic chemistry. Wiley-Interscience, New York
8. Ramamurthy V (1991) Photochemistry in organized and constrained media. VCH, New York
9. Dash N, Chipem SAF, Swaminathan R, Krishnamoorthy G (2008) Hydrogen bond induced twisted intramolecular charge transfer in 2-(4′-N, N-dimethylamino) phenylimidazo[4,5-b]pyridine. Chem Phys Lett 460(1):119–124. doi:10.1016/j.cplett.2008.05.092
10. Novaki PL, El-Seoud AO (1999) Solvatochromism in aqueous micellar solutions: effects of the molecular structures of solvatochromic probes and cationic surfactants. Phys Chem Chem Phys 1 (8):1957–1964. doi:10.1039/A809244C
11. Rekharsky VM, Inoue Y (1998) Complexation thermodynamics of cyclodextrins. Chem Rev 98(5):1875–1917. doi:10.1021/cr970015o
12. Frömming HK, Szejtli J (1994) In: Davies JED (eds) Topics in inclusion science, cyclodextrins in pharmacy. Kluwer Academic Publishers, pp 127–196
13. Busch WK, Swamidoss MI, Fakayode OS, Busch AM (2003) Determination of the enantiomericcomposition of guest molecules by chemometric analysis of the UV-visible spectra of cyclodextrin guest-host complexes. J Am Chem Soc 125(7):1690–1691. doi:10.1021/ja025947a
14. Schneider JH, Hacket F, Rüdiger V, Ikeda H (1998) NMR studies of cyclodextrins and cyclodextrin complexes. Chem Rev 98 (5):1755–1785
15. Bakirci H, Zhang X, Nau MW (2005) Induced circular dichroism and structural bicyclic azoalkanes. J Org Chem 70(1):39–46. doi:10.1021/jo048420k
16. Harata K (1998) Structural aspects of stereo differentiation in the solid state. Chem Rev 98(5):1803–1827. doi:10.1002/chin.199839315
17. Wagner B (2003) In: Nalwa H (ed) Supramolecular photochemistry. American Scientific Publishers, Stevenson Ranch, pp 1–57
18. Lipkowitz BK (1998) Applications of computational chemistry to the study of cyclodextrins. Chem Rev 98(5):1829–1873. doi:10.1021/cr9700179
19. Hu JY, Liu Y, Wang BJ, Xiao HX, Qu SS (2004) Study of the interaction between monoammonium glycyrrhizinate and bovine serum albumin. J Pharm Biomed Anal 36(4):915–919. doi:10.1016/j.jpba.2004.08.021
20. Katrahalli U, Jaldappagari S, Kalanur SS (2010) Study of the interaction between fluoxetine hydrochloride and bovine serum albumin in the imitated physiological conditions by multispectroscopic methods. J Lumin 130(2):211–216. doi:10.1016/j.jlumin.2009.07.033
21. Shaikh TMS, Seetharamappa J, Ashoka S, Kandagal BP (2007) A study of the interaction between bromopyrogallol red and bovine serum albumin by spectroscopic methods. Dyes Pigments 73 (2):211–216. doi:10.1016/j.dyepig.2005.11.008
22. Nagakura S (1975) In: Lim EC (ed) Excited states. Academic, New York, p 322
23. Connolly SJ, Bolton RJ (1990) In: Fox MA, Chanon M (eds) Photoinduced electron transfer. Elsevier, Amesterdam
24. Lueck H, Windsor M, Rettig W (1990) Pressure dependence of the kinetics of photoinduced intramolecular charge separation in 9,9′-bianthryl monitored by picosecond transient absorption: comparison with electron transfer in photosynthesis. J Phys Chem 94 (11):4550–4559. doi:10.1021/j100374a037
25. Panja S, Chakravorti S (2001) Dynamics of twisted intramolecular charge transfer process of 4-N, N-dimethylaminocinnamic acid in a -cyclodextrin environment. Chem Phys Lett 336:57–64. doi:10.1002/jctb.5010150309
26. Lakowicz RJ (1994) Topics in fluorescence spectroscopy, Ed., Plenum Press, New York
27. Basu KJ, Shannigrahi M, Bagchi S (2006) Lithium ion_ketocyanine dye interactions in the ground and excited states. J Phys Chem A 110 (29):9051–9056. doi:10.1021/jp0626081
28. Basu KJ, Shannigrahi M, Bagchi S (2007) Ground and excited state complexation of ketocyanine dyes with alkaline earth metal ions. J Phys Chem A 111(30):7066–7072. doi:10.1021/jp071375a
29. Fayed AT, Awad KM (2004) Dual emission of chalcone-analogue dyes emitting in the red region. Chem Phys 303(3):317–326. doi:10.1016/j.chemphys.2004.06.023
30. Gaber M, El-Daly AS, El-Sayed SY (2008) Spectral properties and inclusion of 3-(4′-dimethylaminophenyl)-1-(2-furanyl)prop-2-en-1-one in organized media of micellar solutions, β-cyclodextrin and viscous medium. Colloid Surf B 66(1):103–109. doi:10.1016/j.colsurfb.2008.05.015
31. Dimroth K, Reichardt C, Siepman T, Bohlman F (1963) Uber pyridinium-N-phenol-betaine und ihre verwendung zur charakterisierung der polaritat von losungsmitteln. Liebigs Ann Chem 661 (1):1–37. doi:10.1002/jlac.19717520109
32. Fayed AT, El-morsi AM, El-Nahass NM (2011) Intramolecular charge transfer emission of a new ketocyanine dye: effects of hydrogen bonding and electrolyte. J Photochem Photobiol A Chem 224(1):38–45. doi:10.1016/j.jphotochem.2011.09.004
33. Saroja G, Samanta A (1995) Polarity of the micelle-water interface as seen by 4-aminophthalimide, a solvent sensitive fluorescence probe. Chem Phys Lett 246(4):506–512. doi:10.1016/0009-2614(95)01131-6
34. Almgren M, Grieser F, Thomas KJ (1979) Dynamic and static aspects of solubilization of neutral arenes in ionic micellar solutions. J Am Chem Soc 101(2):279–291. doi:10.1021/ja00496a001
35. Saroja G, Ramachandan B, Saha S, Samanta A (1999) The fluorescence response of a structurally modified 4-aminophthalimide derivative covalently attached to a fatty acid in homogeneous and micellar environments. J Phys Chem B103(15):2906–2911. doi:10.1021/jp983676d
36. Endo T, Nagase H, Ueda H, Kobayashi S, Nagai T (1997) Isolation, purification, and characterization of cyclomaltotetradecaose (ι-cyclodextirn), cyclomaltopentadecaose (κ-cyclodextrin), cyclomaltohexadecaose (λ-cyclodextrin), and cyclomaltoheptadecaose (μ-cyclodextrin). Chem Pharm Bull 45:532–536. doi:10.1208/pt060243
37. Benesi LM, Hildebrand HJ (1949) A spectrophotometric investigation of the interaction of iodine with aromatic hydrocarbons. J Am Chem Soc 71:2703–2707. doi:10.1021/ja01176a030
38. Lewis NG, Ranadall M (1961) Thermodynamic, 2nd edn. McGrow-Hill Book Company, New York, p 640
39. Bergeron JR (1984) In: Atwood JL, Davies JE, MacNichol DD (eds) Inclusion compounds. Academic, New York, p 423
40. Liu Y, Han HB, Chen TY (2002) Molecular recognition and complexation thermodynamics of dye guest molecules by

modified cyclodextrins and calixarenesulfonates. J Phys Chem B 106(18):4678–4687. doi:10.1021/jp015603r
41. Nilsson M, Valente JA, Olofsson G, Soderman O, Bonini M (2008) Thermodynamic and kinetic characterization of host-guest association between bolaform surfactants and alpha- and beta-cyclodextrins. J Phys Chem B 112(36):11310–11316. doi:10.1021jp802963x
42. Sarkar D, Mahata A, Das P, Girigoswami A, Ghosh D, Chattopadhyay N (2009) Deciphering the perturbation of serum albumins by a ketocyanine dye: a spectroscopic approach. J Photochem Photobiol B 96 (2):136–143. doi:10.1016/j.jphotobiol.2009.05.002
43. Lakowicz RJ (2006) Principles of fluorescence spectroscopy, 3rd edn. Springer, New York, p 954
44. Dewey GT (1991) Biophysical and biochemical aspects of fluorescence spectroscopy. Plenum, New York, pp 1–41
45. Guillet J (1987) Polymer photophysics and photochemistry: an introduction to the study of photoprocesses in macromolecules, p 58
46. Becker OGH (1981) Einfuhrung in die photochemie, 3rd edn. Deutscher Verlag Der Wissenschaften, Berlin
47. Förster T (1965) Delocalized excitation and excitation transfer, modern quantum chemistry. Academic, New York, pp 93–137
48. Cyril L, Earl KJ, Sperry MW (1961) Biochemist's handbook. E. & F.N. Spon, London, p 84
49. Valeur B, Brochon CJ (2001) New trends in fluorescence spectroscopy. Springer, Berlin, p 25
50. Deepa S, Mishra KA (2005) Fluorescence spectroscopic study of serum albumin–bromadiolone interaction: fluorimetric determination of bromadiolone. J Pharm Biomed Anal 38(3):556–563. doi:10.1016/j.jpba.2005.01.023